J|A|C|S COMMUNICATIONS

Published on Web 10/08/2010

Synthesis of Redox Active Ferrocene-Modified Phospholipids by Transphosphatidylation Reaction and Chronoamperometry Study of the Corresponding Redox Sensitive Liposome

Debby Correia-Ledo, Alexandre A. Arnold, and Janine Mauzeroll*

Université du Québec à Montréal, Department of Chemistry, C.P. 8888, Succ. Centre-Ville, Montreal, Quebec, Canada, H3C 3P8

Received July 5, 2010; E-mail: mauzeroll.janine@uqam.ca

Abstract: The design of stable redox active liposomes where the organometallic electroactive pendent was covalently bound to the phospholipid headgroup through a phospholipase D (PLD)-catalyzed transphosphatidylation reaction between a choline-bearing phospholipid and a primary alcohol containing a ferrocene derivative is reported. The functionalization of a liposome surface with this organometallic redox phospholipid allowed the study of membrane-bound electrochemical reactions, which are important in the design of redox-sensitive liposome delivery systems.

Liposomes are biomimetic models that are coveted in drug target and delivery studies because they enable the "smart" delivery of an encapsulated cargo to a target site. Through the combination of stimuli-responsive molecules and phospholipid assemblies, local control over the payload release based on an endogenous or exogenous trigger confers a spatial and temporal specificity, which is highly sought after in the delivery of therapeutics.[1]

Endogenously, pH variations in organelles, the presence of biomarkers, and elevated enzyme activity can supply the required stimuli that triggers the unloading of the liposome payload.[2] Redox-responsive liposomes are inherently interesting delivery systems, since the careful control of the formal potential and ligand environment of the electroactive tethering molecules enable a spontaneous and selective triggering by enzymes, such as reductases, which are found to have a high activity in cancer tissues.[3]

Although surface functionalization strategies are diverse and well established, liposome surface functionalization with electroactive units has been limited to organic[4] or quinone[5−8] based electroactive pendents. For example, Leidner and co-workers[5,6] used phosphatidylcholine anthraquinone based liposomes as chemical models in respiratory and photosynthetic energy transduction studies. They demonstrated that the oxidation or reduction of the electroactive molecules resulted in membrane permeability alterations of the liposome, which is desirable for liposome unloading.

The membrane permeability of liposomes has been studied by HPLC in plastoquinone and ubiquinone imbedded phospholipid liposomes.[7] NMR methods are also well adapted to study the dynamics and overall permeability of liposomes.[9,10] Finally, electrochemical methods are ideally suited for such studies because both liposome dynamics and electroactive tags can be monitored. Nonfaradaic processes, such as capacitive spikes observed in cyclic voltammograms, provide information on liposome fusion dynamics, membrane fluidity, and stability.[2,11,12] Faradaic processes observed as a result of phospholipid functionalization with electroactive units[2] and payload release of redox mediators[13] evaluate the permeability, electron transfer kinetics, and mobility of the electroactive tags.

As quinone-functionalized liposomes are known to be unstable over time, there is a need to design stable tunable redox liposomes, thus extending the range of accessible endogenous redox triggers. As such, the modification of a liposome surface by organometallic pendents is an attractive solution, given the tuneability of the redox formal potential of the tag with the nature of the substituting ligands.

Scheme 1. Schematic Representation of the Synthesis of a Redox Phospholipid, **5a**, **5b**, **6a**, and **6b**, through a PLD-Catalyzed Transphosphatidylation Reaction between a Ferrocene Alcohol Derivative, **3** or **4**, and 1,2-Distearoyl-*sn*-glycero-3-phosphocholine (DSPC), **1**, or 1,2-Dibutyryl-*sn*-glycero-3-phosphocholine, **2**

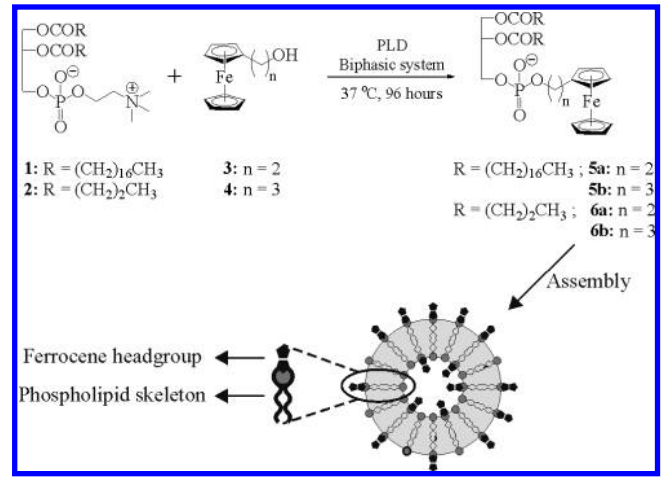

Ferrocene-modified liposomes are ideal biomimetic membrane models that present straightforward electrochemical behavior and stability, as largely documented in two-dimensional self-assembled systems.[14,15] Ferrocene derived compounds have been used in studies involving liposomes but were either imbedded into the lipid membrane or encapsulated into the internal void of the liposome. Lynn and co-workers[16] reported ferrocene-containing cationic lipids used to mediate cell transfection, which is highly dependent upon the oxidation state of the ferrocenyl groups. Also, a specific protein assay system was developed based on functional liposome-modified gold electrodes.[17] Importantly, liposome surface functionalization with organometallic pendents remains unexplored. The only available reported study suffered from severe redox phospholipid instability that prevented the formation of organometallic redox active liposomes.[18] Specifically, the synthesis of a redox active 1,2-distearoyl-*sn*-glycero-3-phosphocholine (DSPC) bearing a ferrocenemethanol function, DSP-OCH_2Fc, resulted in the formation of an unstable product because the redox headgroup underwent hydrolysis and/or S_N2 reactions, which favored the formation of phosphatidic acid. To overcome this limitation, it was hypothesized that increasing the length of the alkyl chain between the phosphorus

10.1021/ja105921g

and the ferrocene group should further stabilize the redox active phospholipid product.

Herein, we report the design of stable redox active liposomes where the organometallic electroactive pendent was covalently bound to the phospholipid headgroup through a phospholipase D (PLD)-catalyzed transphosphatidylation reaction between a choline-bearing phospholipid, **1** or **2**, and a primary alcohol containing a ferrocene derivative, **3** or **4** (Scheme 1). This reaction appears to be robust and would be widely applicable as demonstrated by the application to phospholipids with varying alkyl chain lengths and two different ferrocene derivatives.

Purification of the reaction mixture was limited to the separation of the phospholipids from the enzyme and excess of alcohol. No further purification was needed since DSPC is needed once more for the liposome formation through the double emulsion technique. The redox phospholipid, DSP-OCH_2CH_2Fc, characterization and DSPC/DSP-OCH_2CH_2Fc ratio quantification were achieved through solid-state phosphorus NMR (Figure 1). The study of phospholipids by solid-state ^{31}P NMR is a well established technique.[19−21] Spectral analysis is greatly simplified with respect to ^{1}H NMR since each phospholipid contains a single phosphorus atom per headgroup. In addition, speciation is possible because the headgroup modification with a ferrocene derivative, a well-known electron donor, is likely to alter the shielding of the ^{31}P nucleus and, thus, its chemical shift. It is important to mention that the ^{1}H NMR could not be acquired since the lipid mixture, DSPC/DSP-OCH_2CH_2Fc, proved to be insoluble in the usual deuterated solvents used for phospholipid NMR studies, such as chloroform, ethanol, dichloromethane, and even a chloroform/ethanol (2/1) mixture.[22]

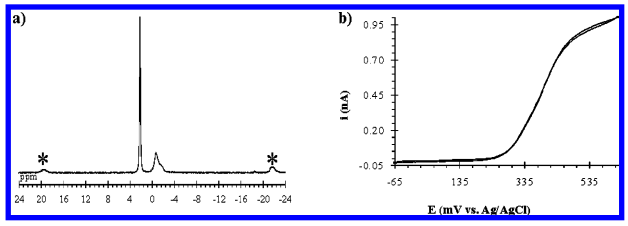

Figure 1. (a) Magic-angle spinning ^{31}P NMR solid-state spectra of a DSPC/DSP-OCH_2CH_2Fc 1:0.6 mixture with a MAS of 5 kHz. Spinning sidebands are identified by *. A 3 s recycle delay was used between acquisitions to allow full relaxation of the NMR signal. (b) Cyclic voltammogram (CV) of 1 mM DSP-OCH_2CH_2Fc solution in 0.1 M tetrabutylammonium tetrafluoroborate solution in acetonitrile. CVs were recorded at a platinum 25 μm diameter microelectrode at a 10 mV/s scan rate.

When hydrated, phospholipids adopt different morphologies such as multilamellar vesicles (MLVs), small unilamellar vesicles (SUVs), or micelles. In static spectra, objects which slowly reorient themselves in the magnetic field, such as MLVs, display broad ^{31}P spectra that reflects the chemical shift anisotropy interaction.[19−21] In contrast, small objects that reorient rapidly, such as SUVs or micelles, display spectra composed of sharp peaks akin to those obtained in liquid-state NMR. The ^{31}P chemical shift anisotropy is averaged out by Magic-Angle Spinning (MAS) of the sample at a 54.7° angle with respect to the magnetic field, where the resulting spectra now present a set of spinning sidebands with relative intensities representative of the chemical shift interaction tensor.[23]

Figure 1a displays the MAS spectrum at 5 kHz spinning. It is composed of a sharp peak at 2.18 ppm and a spinning sideband manifold centered at −0.77 ppm. The spinning sideband spectrum and its isotropic chemical shift (−0.77 ppm) are typical of MLVs of phospholipids and are assigned to unmodified DSPC. The chemical shift of the single resonance (2.18 ppm) is assigned to the DSP-OCH_2CH_2Fc. No spinning sidebands corresponding to this peak were observed, and this same sharp peak was also present in the static spectrum (data not shown). Thus, it appears that DSP-OCH_2CH_2Fc forms small isotropic objects such as micelles or SUVs that rapidly reorient in the magnetic field. Providing that the NMR signal is allowed to fully relax between acquisitions, the ^{31}P solid-state NMR peaks can be used to quantify the yield of the transphosphatidylation reaction. A 1:0.6 DSPC/DSP-OCH_2CH_2Fc ratio was determined by integrating the single DSP-OCH_2CH_2Fc peak and the spinning sideband DSPC manifold.

Similar NMR results and reaction yields were obtained by replacing the ferrocene-ethanol tether with ferrocene-propanol. The MAS spectrum presents a broad peak at −0.27 ppm flanked by spinning sidebands, which again can be assigned to unmodified DSPC. A second peak was also observed at 2.04 ppm with no spinning sidebands thus suggesting that DSP-$OCH_2CH_2CH_2Fc$ also forms micelles. We tentatively attribute the small increase in DSPC chemical shift to the presence of a small fraction of DSP-$OCH_2CH_2CH_2Fc$ within the bilayer, an effect which has been observed when charged molecules perturb the bilayer.[24]

The synthesized redox modified phospholipids present stable electroactive behaviors as presented in the representative cyclic voltammogram of DSP-OCH_2CH_2Fc (Figure 1b). As expected, pendent substitutions of organometallic complexes lead to an anodic shift of the standard potential from 249 mV for ferrocene-ethanol to 374 mV for DSP-OCH_2CH_2Fc in acetonitrile.[25] Using the respective cyclic voltammograms and considering that ferrocene oxidation/reduction process is a standard reversible one-electron transfer process,[26] the diffusion coefficients of the redox phospholipids were determined. A value of 3.2×10^{-5} cm^2/s was determined for ferrocene-ethanol in acetonitrile, and a diffusion coefficient of 1.9×10^{-6} cm^2/s for DSP-OCH_2CH_2Fc was observed under the same conditions. The increased molecular weight of DSP-OCH_2CH_2Fc, as compared to ferrocene-ethanol, leads to a decrease in its diffusion coefficient, which resulted in a decrease of the anodic steady-state current.

The covalent nature of the ferrocene unit attachment to the phospholipid headgroup was supported by infrared analysis. In the 3000 cm^{-1} region, DSPC has a ν(C−H) band at 3376 cm^{-1}, which is consistent with literature.[27] In the same region, DSP-OCH_2CH_2Fc has an additional contribution assigned to the ν(C−H) at 3231 cm^{-1} band of the ferrocene unit. Also, the two low intensity ferrocene ring modes,[27] not present in the DSPC spectra, are observed in the DSP-OCH_2CH_2Fc spectra at 605 and 1400 cm^{-1}. Finally and most importantly, the redox DSPC spectra of ν(P═O) at 1236 cm^{-1} is 20 cm^{-1} downshifted as compared to the DSPC phosphorus band, which is at 1254 cm^{-1}. This shift is significant and indicative of a phospholipid headgroup modification. It is expected that the zwitterionic character of the choline function present in the DSPC allows for a six-member-like reorganization that will not occur once the choline has been replaced by the ferrocene unit, and this results in a shift of the expected P═O mode.[27]

On the MS spectrum, m/z [M + H^+] 912 and m/z [M + Na^+] 934 were attributed to DSP-OCH_2CH_2Fc. A comparison with the expected m/z exhibits a four unit difference that is thought to be related to post-transphosphatidylation activity of the PLD or to a gas phase reaction during the ionization process. The same four unit discrepancy was also observed when 1,2-dibutyryl-*sn*-glycero-3-phosphocholine, which presents shorter alkyl chains, was used instead of the DSPC.

Having synthesized and characterized stable electroactive phospholipids, the formation of a redox active liposome was achieved from a double emulsion technique using a DSPG, DSPC, and DSP-OCH_2CH_2Fc mixture. Using the yield obtained from the transpho-

sphatidylation reaction determined by ^{31}P NMR, the surface concentration of reduced ferrocene units exposed to the external solution on a single redox liposome could be at most 15%. Given their probable partition in both leaflets of the membranes, redox units are considered quite dilute, which suggests that neighboring effects following oxidation are negligible.

To promote liposome immobilization at the bottom of the electrochemical cell during chronoamperometry, sucrose ($\rho = 1.59$ g/cm^3) was added into the internal void of the liposomes. Since glucose ($\rho = 1.54$ g/cm^3) is added to the electrolyte solution, liposome sedimentation is based on the differential density of the respective sugars. Figure 2a and 2b present the optical micrographs of a large stable liposome (100−250 μm diameter), which enabled single liposome monitoring when using a conventional microelectrode tip (25 μm diameter Pt).

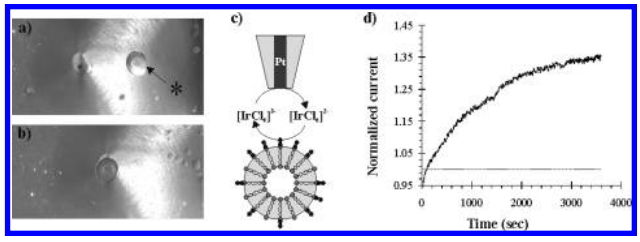

Figure 2. Optical micrographs presenting (a) the microelectrode adjacent to a liposome (*) and (b) the microelectrode positioned above the liposome. (c) Schematic representation of the oxidation of $[IrCl_6]^{3-}$ at a microelectrode whereby $[IrCl_6]^{2-}$ is produced and diffuses to the immobilized liposome surface where it oxidizes the ferrocene headgroups. (d) Chronoamperometry measurements over a bare liposome (---) and a redox liposome (—). The current vs time curves were recorded at a platinum 25 μm diameter microelectrode in a 1 mM K_3IrCl_6 solution/50 mM glucose/0.1 M KCl aqueous solution at a tip to liposome distance of 20 μm.

To established the redox activity of the resulting liposomes, the reduced ferrocene headgroups were oxidized using a sacrificial redox couple, $[IrCl_6]^{3-/2-}$.[28,29] Thermodynamically, the electron transfer between ferrocene moieties of the liposome and $[IrCl_6]^{3-}$ is favorable.[28] In the context of a Scanning Electrochemical Microscopy (SECM) experiment, $[IrCl_6]^{3-}$ is oxidized at a microelectrode positioned directly above the liposome. $[IrCl_6]^{2-}$ diffuses to the surface of the liposome where it is spontaneously reduced back to $[IrCl_6]^{3-}$ by the ferrocene units anchored at the surface of the liposome. $[IrCl_6]^{3-}$ diffuses back to the tip to produce an enhancement oxidized current measured at the microelectrode (Figure 2c). This enhanced material flux only occurs for short microelectrode to liposome distances characteristic of the feedback mode of SECM.

The chronoamperometric measurements described above were carried out on control liposomes, devoid of DSP-OCH_2CH_2Fc. Based on the $[IrCl_6]^{3-}$ cyclic voltammetry, an applied mass transport limited bias ranging from 850 to 875 mV was consistently used during the chronoamperometry measurements of both liposomes. The microelectrode to liposome distance at which the current time profile was measured was kept at 20 μm. The response of the control liposome provided a background response that was used to normalize the response observed at the redox liposomes. Figure 2d presents the normalized current response of the control and redox liposomes. The response measured at the control liposome is unaffected by the presence of the oxidized species, $[IrCl_6]^{2-}$, generated at the nearby microelectrode. In contrast, the surface of the redox liposome is electroactive and reacts with the $[IrCl_6]^{2-}$ species that diffuses in the cleft to the microelectrode surface, which regenerates the $[IrCl_6]^{3-}$ species. This regeneration reaction occurs and produces an additional flux of $[IrCl_6]^{3-}$ species, within a few microseconds, that yields an increase in the current measured at the microelectrode. It is noteworthy that the chronoamperometric curve seems to stabilize over time and reach a stable turnover rate. At longer experimental times, the current stabilization cannot be maintained with the depletion of the surface available ferrocene units and a decrease in current returning to baseline is expected. This is however rarely observed because the liposomes burst as a result of either osmolality variations that occur with solution evaporation or membrane permeability alterations leading to liposome unloading.

To evaluate the extent of the regeneration reaction of $[IrCl_6]^{3-}$ by the tethered ferrocene phospholipids, classical feedback approach curves were performed over a single immobilized redox liposome using a platinum 25 μm diameter microelectrode. The resulting curve (Figure 3, black line) was normalized by the steady-state current observed at large tip to substrate distances. Comparison of the experimental approach curve to pure negative feedback theory (Figure 3, dash line) reveals a deviation between the two curves at tip to substrate distances below 2. The increased feedback response of the redox liposome as compared to pure negative feedback behavior confirms the presence of a regeneration reaction between K_3IrCl_6 and the ferrocene units covalently bound to the phospholipid headgroup. Extraction of quantitative kinetic parameters from the present approach curve is not straightforward and therefore outside the scope of the present work. It will require the development of validated numerical simulations based on a model which considers at the very least substrate and tip geometry as well as the availability and mobility of the redox phospholipids between leaflets and during the regeneration reaction.

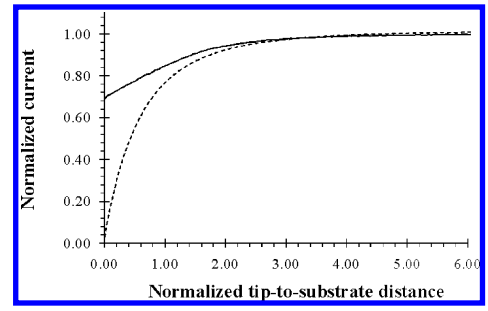

Figure 3. Approach curve obtained over a single immobilized surface-modified ferrocene liposome (—) and compared to pure negative feedback (---). The approach curve was performed using a platinum 25 μm diameter microelectrode in a 1 mM K_3IrCl_6 solution in a 50 mM glucose and 0.1 M KCl aqueous solution.

In summary, we present a broadly applicable synthesis of stable organometallic modified phospholipids through the covalent attachment of ferrocene-primary alcohols to choline-bearing phospholipids using an enzymatic transphosphatidylation reaction. The functionalization of a liposome surface with this organometallic phospholipid allows the study of the electrochemical activity of the liposome with time using K_3IrCl_6. The development of this general simple synthetic pathway enabling attachment of organometallics containing primary alcohols will allow in-depth studies of membrane-bound electrochemical reactions, which are important to the successful design of specific redox-sensitive liposome delivery systems. Undoubtedly, the membrane permeability alteration events leading to liposome unloading will depend on the electron transfer rate and surface concentration of organometallic phospholipids. The apparent electron transfer rate will be affected by the nature of the redox center (iron, osmium, ruthenium for example), its immediate chemical environment (Coulombic interactions between organometallic moieties, so-called neighboring effect[15]), its accessibility, and solvation. The methodology described herein will

not only enable systematic studies of such tunable parameters but also address critical interrogations such as the critical ratio of redox modified lipid to unmodified lipid required for a successful liposome release following a specific endogenous or exogenous trigger. Finally, through directed ligand substitution, an expansion of the formal potential of the stimuli-responsive unit used in the context of redox liposome delivery systems will be possible, thus broadening the range of accessible enzymes that can endogenously trigger liposome payload release.

Acknowledgment. The authors acknowledge the Natural Sciences and Engineering Research Council of Canada (NSERC), the Canada Foundation for Innovation (CFI), the Center for Self-Assembled Chemical Structures (CSACS), the Fonds Québécois de la Recherche sur la Nature et les Technologies (FQRNT), the Centre Québécois sur les Matériaux Fonctionnels (CQMF), and NanoQAM for their financial support. Dr. Sylvain Canesi and Noémie Wezel are also acknowledged for conceptual and technical contributions respectively.

References

(1) Dreher, M. R.; Chilkoti, A. *J. Natl. Cancer Inst.* **2007**, *99*, 983.
(2) Hellberg, D.; Scholz, F.; Schubert, F.; Lovric, M.; Omanovic, D.; Hernandez, V. A.; Thede, R. *J. Phys. Chem. B* **2005**, *109*, 14715.
(3) Fitzsimmons, S. A.; Workman, P.; Grever, M.; Paull, K.; Camalier, R.; Lewis, A. D. *J. Natl. Cancer Inst.* **1996**, *88*, 259.
(4) Wang, P.; Schuster, M.; Wang, Y. F.; Wong, C.-H. *J. Am. Chem. Soc.* **1993**, *115*, 10487.
(5) Liu, M. D.; Patterson, D. H.; Jones, C. R.; Leidner, C. R. *J. Phys. Chem.* **1991**, *95*, 1858.
(6) Leidner, C. R.; Liu, M. D. *J. Am. Chem. Soc.* **1989**, *111*, 6859.
(7) Jemiota-Rzeminska, M.; Latowski, D.; Strzalka, K. *Chem. Phys. Lipids* **2001**, *110*, 85.
(8) Ong, W.; Yang, Y.; Cruciano, A. C.; McCarley, R. L. *J. Am. Chem. Soc.* **2008**, *130*, 14739.
(9) Ouellet, M.; Otis, F.; Voyer, N.; Auger, M. *Biochim. Biophys. Acta* **2006**, *1758*, 1235.
(10) Auger, M. *Curr. Issues Mol. Biol.* **2000**, *2*, 119.
(11) Hernandez, V. A.; Scholz, F. *Langmuir* **2006**, *22*, 10723.
(12) Hernandez, V. A.; Scholz, F. *Isr. J. Chem.* **2008**, *48*, 169.
(13) Zhan, W.; Bard, A. *J. Anal. Chem.* **2006**, *78*, 726.
(14) Lee, L. Y. S.; Sutherland, T. C.; Rucareanu, S.; Lennox, R. B. *Langmuir* **2006**, *22*, 4438.
(15) Norman, L. L.; Badia, A. *J. Am. Chem. Soc.* **2009**, *131*, 2328.
(16) Jewell, C. M.; Hays, M. E.; Kondo, Y.; Abbott, N. L.; Lynn, D. M. *Bioconjugate Chem.* **2008**, *19*, 2120.
(17) Lee, H. Y.; Jung, H. S.; Fujikawa, K.; Park, J. W.; Kim, J. M.; Yukimasa, T.; Sugihara, H.; Kawai, T. *Biosens. Bioelectron.* **2005**, *21*, 833.
(18) Correia-Ledo, D.; Mauzeroll, J. *ECS Trans.* **2009**, *19*, 1.
(19) Seelig, J. *Biochim. Biophys. Acta* **1978**, *515*, 105.
(20) Seelig, J.; Seelig, A. *Q. Rev. Biophys.* **1980**, *13*, 19.
(21) Smith, I. C.; Ekiel, I. H. In *Phosphorus-31 NMR: Principles and Applications*; Gorenstein, D. G., Ed.; Academic Press, Inc.: London, 1984; p 447.
(22) Sotirhos, N.; Herslöf, B.; Kenne, L. *J. Lipid Res.* **1986**, *27*, 386.
(23) Schmidt-Rohr, K.; Spiess, H. W. *Multidimensional Solid-State NMR and Polymers*; Academic Press: Toronto, Canada, 1994.
(24) Bonev, B.; Watts, A.; Bokvist, M.; Gröbner, G. *Phys. Chem. Chem. Phys.* **2001**, *3*, 2904.
(25) Davis, W. L.; Shago, R. F.; Langner, E. H. G.; Swarts, J. C. *Polyhedron* **2005**, *24*, 1611.
(26) Tsierkevos, N. G. *J. Solution Chem.* **2007**, *36*, 289.
(27) Popenoe, D. D.; Deinhammer, R. S.; Porter, M. D. *Langmuir* **1992**, *8*, 2521.
(28) Nijhuis, C. A.; Sinha, J. K.; Wittstock, G.; Huskens, J.; Ravoo, B. J.; Reinhoudt, D. N. *Langmuir* **2006**, *22*, 9770.
(29) Ludden, M. J. W.; Sinha, J. K.; Wittstock, G.; Reinhoudt, D. N.; Huskens, J. *Org. Biomol. Chem.* **2008**, *6*, 1553.

JA105921G